American Mineralogist, Volume 78, pages 178–186, 1993

Activity-composition relationships in the system Fe-Pt at 1300 and 1400 °C and at 1 atm and 20 kbar

GISLI GUDMUNDSSON
Department of Geology, Arizona State University, Tempe, Arizona 85287, U.S.A.
and Department of Geology, University of Bristol, Bristol BS8 1RJ, U.K.

JOHN R. HOLLOWAY
Departments of Geology and Chemistry, Arizona State University, Tempe, Arizona 85287, U.S.A.

ABSTRACT

Activity-composition relationships in the system Fe-Pt have been determined at 1300 and 1400 °C and at 1 atm and 20 kbar. The 1-atm data were fitted to a Redlich-Kister solution model. The activity coefficient of Fe in Fe-Pt alloy is adequately described by log $\gamma_{Fe} = (1 - X_{Fe})^2[B + C(4X_{Fe} - 1)]$, where, at 1400 °C, $B = -3.579$ and $C = -0.151$ and, at 1300 °C, $B = -4.202$ and $C = -0.323$. The fit to the measured activity coefficients (γ_{Fe}) is within ±6.5%. The partial molar volume of Fe in Fe-poor alloys exhibits a substantial negative deviation from ideality. With increasing Fe content (about $X_{Fe} = 0.15$), the volume-composition relationships cross over and show a positive deviation from ideality. In the X_{Fe} range from 0.1 to about 0.35, however, the partial molar volume of Fe in the alloy remains constant, which makes the correction for the effect of pressure on the activity coefficient relatively simple. With increasing Fe content, the volume-composition relationships are likely to become ideal.

Knowledge of the activity-composition relationships in the system Fe-Pt can be used to measure f_{O_2} in high-pressure experiments with an appropriate phase assemblage such as olivine + orthopyroxene + Fe-Pt metal. The overall accuracy of this method was checked at 1 atm. Using the expression for the activity coefficient of Fe in Fe-Pt alloys given above, calculated f_{O_2} was found to be accurate to within ±0.2 $\log_{10}$ units.

INTRODUCTION

Understanding the activity-composition relationships in the Fe-Pt system is of fundamental importance to experimental geochemistry. The activity of Fe in a melt that is in equilibrium with an Fe-Pt alloy can be obtained directly from the activity-composition relationships of the alloy. Because of the very low solubility of Pt in silicate melts, use of this alloy system does not change the major-element composition of the melt. Given suitable coexisting phases, the value for the activity of Fe in the melt can in turn be used to calculate f_{O_2} using, for instance, coexisting (Fe-alloy)-orthopyroxene-olivine to estimate f_{O_2}, as has been done by Bertka and Holloway (1988), Gudmundsson et al. (1988), and Jamieson et al. (1992).

The system Fe-Pt has rather complex subsolidus relations below 1200 °C, but between approximately 1300 °C and the solidus there is a single-phase solution with a very shallow eutectic at a very low concentration of Pt in the alloy (e.g., Hultgren et al., 1973). The tendency of Fe to alloy with Pt has been known for several decades and has posed serious problems to experimental petrologists because it results in Fe loss to Pt sample containers (e.g., Ito and Kennedy, 1967; Merrill and Wyllie, 1973). As pointed out by Grove (1981), this loss is a result of the large negative deviation from ideality in the Fe-Pt system, which leads to a high concentration of Fe in Pt, even at low Fe activities. Therefore, a starting material in a high-temperature experiment may lose some, or even all, of its Fe to the Pt container. The degree of the depletion depends on temperature, f_{O_2}, initial composition, duration, and pressure, as well as the volumetric ratio of sample to metal (Stern and Wyllie, 1975). Values of reported Fe loss range from almost none to almost complete. Yoder and Tilley (1962) report only 2% Fe loss, whereas Green and Ringwood (1967, 1970) found that in their experiments the total Fe loss ranged from 20 to 40%. Merrill and Wyllie (1973) reported a 97% Fe loss in their experiments.

Reduction of Fe loss can be accomplished by the use of capsule materials other than pure Pt, such as Ag, Au, Ag-rich Ag-Pd, Mo, Fe, or Fe-Pt. Unfortunately, all these metals or alloys have limitations. Noble metals like Ag and Au have fairly low melting points (960, 1064 °C) and so does the Ag-rich portion of the AgPd solid solution, making them unsuitable for critical temperature ranges. Mo has been used as a capsule material (Biggar, 1970; Agee and Walker, 1988), but Mo is not stable under oxidizing conditions. Pure Fe has also been used as a capsule (Ito and Kennedy, 1967) in experiments, but its use often results in the charge gaining rather than losing Fe. Graphite capsules (e.g., Ito and Kennedy, 1967; Taka-

0003–004X/93/0102–0178$02.00

hashi and Kushiro, 1983) may eliminate Fe loss, but the f_{O_2} conditions possible in the presence of graphite are limited, and melts always contain some dissolved CO_2 (Holloway et al., 1992). One way in which Pt may be used is by controlling its initial Fe content, for example, electroplating with Fe to prevent Fe loss (Johannes and Bode, 1978). Alternatively the capsule (or the Pt wire, in 1-atm experiments) can be presaturated with Fe (Ford, 1978; Grove, 1981). For a high-pressure experiment, determination of the appropriate level of presaturation requires knowledge of f_{O_2} conditions and of the activity-composition relationships in the alloy. The aims of this study were to determine Fe-Pt activity-composition relationships in order that Fe concentration may be used as an O sensor in 1-atm and high-pressure experiments and to estimate levels of Fe saturation required in high-pressure experiments.

Previous work

Activities in the Fe-O system

Calculation of the activity of Fe in Pt in equilibrium with iron oxides relies on knowledge of the activity of Fe in the oxide phases (Darken and Gurry, 1945, 1946). The system Fe-O is characterized by the existence of nonstoichiometric phases, in particular wüstite, whose atomic ratio of O to Fe ranges from ~1.05 to ~1.19.

Since the effect of f_{O_2} on the composition of wüstite is known, the activity of Fe in wüstite or any Fe-O complex can be derived by means of a Gibbs-Duhem integration (Darken and Gurry, 1945) with Fe in equilibrium with wüstite as the standard state

$$\mathrm{d}\log a_{Fe} = -\int N_O/N_{Fe}\,\mathrm{d}\log_{10} fO_2^{1/2} \qquad (1)$$

where N_O and N_{Fe} are the atomic fraction of Fe and O, respectively, f_{O_2} is the oxygen fugacity, and a_{Fe} is the activity of Fe.

Activity composition relations in the system Fe-Pt

Larson and Chipman (1954) studied the activity of Fe in Fe-Pt alloys at 1550 °C and 1 atm by equilibrating Pt with lime-Fe slags at known f_{O_2}. Taylor and Muan (1962) and Heald (1967) investigated the system Fe-Pt-O at 1300 °C and at 1131–1348 °C, respectively, under controlled f_{O_2} conditions at 1 atm. Larson and Chipman (1954) and Heald (1967) determined the composition of their product alloys by wet chemistry, whereas Taylor and Muan (1962) derived their compositions by measuring the weight change of the sample during the experiments.

If Pt is equilibrated with iron oxide, the chemical potential of Fe in the resulting Fe-Pt alloy is the same as the chemical potential of Fe in the coexisting iron oxide, and it can therefore be calculated through Gibbs-Duhem integration if f_{O_2} is known (Eq. 1). The activity coefficients of Fe in Fe-Pt alloy as a function of composition calculated in this manner by Taylor and Muan (1962) and Heald (1967) are shown in Figure 1. Heald (1967) fitted his data and the data of Taylor and Muan (1962)

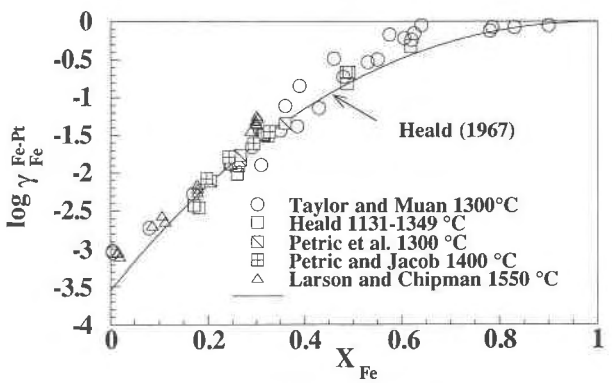

Fig. 1. Activity coefficient of Fe in Fe-Pt alloys vs. mole fraction of Fe. The solid line shows the model of Heald (1967).

to a Redlich-Kister solution model (Redlich and Kister, 1948; described in a following section) by averaging data from all temperatures (1131–1348 °C). Petric et al. (1981) and Petric and Jacob (1982) performed experiments at 1300 and 1400 °C at moderately high f_{O_2}, in which Pt was equilibrated with magnetite. By assuming unit activity of magnetite, they were able to derive a linear expression for the activity coefficient of Fe in Pt as a function of composition. Direct comparison can only be made between the data of Taylor and Muan (1962) and Heald (1967), since these studies used the same standard state, i.e., Fe in equilibrium with wüstite. Petric et al. (1981) and Petric and Jacob (1982) used the same standard state but adopted a calibration of the Fe + wüstite buffer from Spencer and Kubaschewski (1978), which makes the activity coefficient about 0.10 of a $\log_{10}$ unit more negative. However, Larson and Chipman (1954) used pure liquid Fe as a standard state, which is much different and not easily comparable to the Fe + wüstite equilibria. Comparison between the work of Taylor and Muan (1962) and Heald (1967) shows that, at low concentration of Fe in the Fe-Pt alloy, the Redlich-Kister model of Heald (1967) deviates considerably from the data of Taylor and Muan (1962).

Experimental procedures and analytical techniques

Gas-mixing apparatus

Experiments at 1 atm were performed in a vertical gas-mixing furnace with silicon carbide heating elements. The temperature was read with a Pt-$Pt_{90}Rh_{10}$ thermocouple, situated a few millimeters above the sample. The thermocouple was calibrated against the melting points of Au (1064 °C) and diopside (1391 °C).

In most of the experiments, f_{O_2} was set by a mixture of CO_2 and CO that was passed through the furnace at a flow of 4.4 cc/s (Darken and Gurry, 1945). The flow of each component was controlled by a needle valve and measured with a flow meter. The CO_2/CO ratio fixes the f_{O_2} at a given temperature, and the value of f_{O_2} was calculated from the data given by Robie et al. (1978). The

TABLE 1. Gas-mixing experiments

Expt.	T (°C)	log f_{O_2}	Duration (h)	Starting material
6	1400	−4.5	7	Pt, Fe_2O_3
8	1400	−7.5	60	Pt, Fe_2O_3
11	1400	−0.68	48	Pt, Fe_2O_3
12	1400	−9.0	50	Pt, Fe
13	1400	−8.5	47	Pt, Fe_2O_3
15	1400	−8.5	68	Pt, Fe
16*	1400	−5.40	22	Pt, Fe_2O_3
17*	1400	−8.57	22	Pt, Fe_2O_3
18	1300	−6.0	51	Pt, Fe_2O_3, Fe-Pt
20 a,b	1400	−0.68	91	Pt, Fe_2O_3, Fe-Pt
Vol. 1	1400	−6.0	140	Pt foil, Fe
Vol. 2	1400	−5.0	172	Pt foil, Fe
Vol. 3	1400	−7.5	285	Pt foil, Fe
Vol. 4a,b	1400	−0.68	170	Pt foil, Fe
21a,b	1400	−2.54	175	Pt-Fe, Fe_2O_3
22a,b	1300	−2.54	168	Pt, Fe, Fe-Pt
23a,b	1400	−4.8	45	Pt, Fe, Fe-Pt
24a,b	1300	−5.5	49	Pt, Fe, Fe-Pt

Note: Pt = Pt wire or powder, Fe = Fe powder, Fe_2O_3 = ferric oxide powder, Fe-Pt = Fe-Pt alloy with an initial composition of $X_{Fe}^{Fe\text{-}Pt} = 0.32$.
* Performed at the University of Arizona.

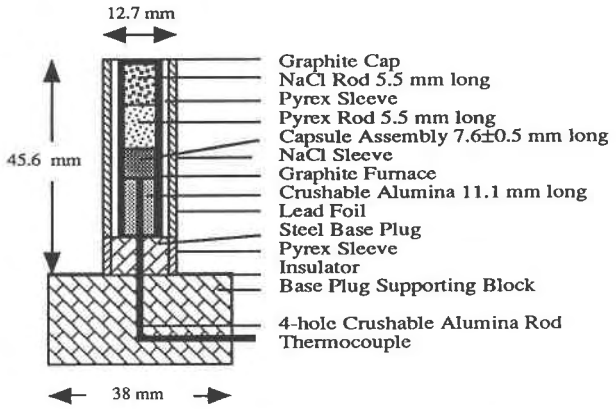

Fig. 2. Cross-sectional view of the piston-cylinder solid-media cell assembly.

f_{O_2} of given CO_2/CO ratios were cross-calibrated to within ± 0.1 $\log_{10}$ units at the nickel + nickel oxide (NNO) buffer (from O'Neill, 1987a). In two experiments (21 and 22) premixed O_2 and Ar gas was passed through the furnace. The furnace was kept open to the atmosphere in experiments 11 and 20 and in experiment vol. 4a,b compressed air flowed through the furnace. Finally, two experiments (16 and 17) were performed in M. J. Drake's laboratory, at the University of Arizona. In these experiments, the f_{O_2} was controlled by CO_2 and H_2 mixtures and its value measured by a ZrO_2 O sensor (e.g., Sato, 1970). These last two experiments were conducted to obtain an interlaboratory comparison with our results.

The samples consisted of various combinations of Pt (99.99% purity) wire, or powder and metallic Fe powder (99.99% purity) or ferric oxide powder (99.99% purity). Reversals were done by replacing the Pt with an Fe-Pt alloy. In four experiments (vol. 1, 2, 3, and 4a,b) a Pt foil (2 × 4 × 0.13 mm) was loaded into a Pt crucible surrounded with Fe powder and hung onto the thermocouple rod.

The experiments were carried out at 1300 and 1400 °C, with the majority of experiments at 1400 °C. Log f_{O_2} ranged from −9.0 to −0.68. All the charges were drop quenched into a H_2O bath, with a typical quench rate of ≥1000 °C/s. Details of experimental conditions are given in Table 1.

Piston cylinder

All the experiments above 1 atm were performed in a piston-cylinder apparatus 12.7 mm in diameter that was not endloaded (Patera and Holloway, 1978). The solid-media assembly (shown in Fig. 2) consisted of a NaCl sleeve, Pyrex glass sleeve, and graphite furnace. The sample container was placed in the center of the graphite furnace. The space below the Pt capsule was filled with crushable alumina, and the capsule was topped with an alumina wafer to prevent the thermocouple from touching or piercing it. The thickness of the wafer was about 0.5 mm. The space between the capsule and the graphite furnace was filled with Pyrex powder, and the space above the sample container was filled with stacked Pyrex and NaCl rods of identical length. The temperature was measured and controlled with a WRe_5-WRe_{26} thermocouple. No correction for the effect of pressure was made on the emf output of the thermocouple. The reported temperature is believed to be precise to ±5 °C. The composition of one thermocouple was checked after an experiment and was found to be unchanged.

During the experiment a piston-out technique was employed. The pressure was initially raised to between 10 and 20% higher than the final value, the temperature was then increased to that desired and then pressure was reduced to the intended value. The measured pressure is believed to be accurate to ±0.5 kbar (Esperanca and Holloway, 1986). All the samples were quenched isobarically. A typical quench rate was about 100 °C/s.

The sample consisted of a solid buffer, either wüstite + magnetite (WM) or magnetite + hematite (MH) + Pt. The oxide phases were made from 99.99% pure Fe powder and were mixed with pure (99.99%) Pt wire or a thin layer of Pt powder. Reversals were made by replacing the Pt layer with an Fe-Pt foil that had higher Fe concentration than was expected at experimental conditions. The sample was loaded into a Pt capsule and welded shut. Detailed experimental conditions are given in Table 2. After each experiment, the sample was checked to ensure that both the buffer phases were still present.

The values for the f_{O_2} in these experiments were calculated using the 1-atm calibration used by O'Neill (1988) for the WM buffer and used by Blumenthal and Whitmore (1961) for the MH buffer. Corrections to high pressures were made using volumes, thermal expansions, and isothermal compressibilities from Berman (1988), except for wüstite. Thermal expansion of wüstite was calculated from the data given in Taylor (1984), and the isothermal

TABLE 2. High pressure experiments

Expt.	T (°C)	log f_{O_2}	Duration (h)	Starting material
P.C. 7	1300	−1.14	25.2	Pt, MH
P.C. 9	1400	−0.17	26.2	Fe-Pt, MH
P.C. 10	1300	−1.14	23.8	Fe-Pt, MH
P.C. 14a,b	1300	−6.66	7.5	Pt, Fe-Pt, WM
P.C. 17a,b	1400	−5.44	21.6	Pt, Fe-Pt, WM

Note: Pt = Pt wire or powder, Fe-Pt = Fe-Pt alloy with an initial composition of $X_{Fe}^{Fe\text{-}Pt} = 0.32$, MH = magnetite-hematite oxides, WM = wüstite-magnetite oxides.

compressibility was adopted from Jeanloz and Hazen (1983).

Analytical methods

The experimental samples were mounted on glass slides, sectioned with a diamond blade, and polished with diamond powder.

Crystalline material was identified by a combination of reflected light microscopy and backscattered electron imaging with a scanning electron microscope (SEM). Quantitative analyses of major elements were performed with a Jeol JXM-8600 electron microprobe, equipped with both wavelength- and energy-dispersive systems. The sample current was 10 nA and the accelerating potential was 20 kV. The crystalline phases were analyzed with a 2-μm beam. In the core of the Fe-Pt alloys, it was necessary to put the beam a distance of at least 20 μm from the edge of the grain because of the excitation of Fe in the surrounding oxide. Because of this problem, the Fe-Pt alloys were, when possible, physically separated from the iron oxides and mounted in epoxy to remove the extra signal from the surroundings. The raw counts were reduced using the ZAF correction method (Reed, 1975).

XRD analysis

The diffractometer was operated with Cu$K\alpha$ radiation at 50 kV and 30 mA with a scan speed of 0.5°/min. Each sample was scanned from 3 to 140°, which included all the major peaks. All the samples contained an internal standard, metallic Si, against which the raw spectra were corrected.

EXPERIMENTAL RESULTS

The Fe contents of the Fe-Pt alloys for each experiment are shown in Table 3 along with 1 sd of the corresponding value, based on accumulated microprobe analyses of individual Fe-Pt grains in the sample. The activity coefficient, also shown in Table 3, was calculated from the relationship

$$\gamma_{Fe}^{Fe\text{-}Pt} = \frac{a_{Fe}^{Fe\text{-}Pt}}{X_{Fe}^{Fe\text{-}Pt}} \quad (2)$$

where $a_{Fe}^{Fe\text{-}Pt}$, $\gamma_{Fe}^{Fe\text{-}Pt}$, and $X_{Fe}^{Fe\text{-}Pt}$ are the activity, activity coefficient, and the mole fraction of Fe in the Fe-Pt alloy, respectively.

TABLE 3. Experimental results

Expt.	$X_{Fe}^{Fe\text{-}Pt}$	sd	log $\gamma_{Fe}^{Fe\text{-}Pt}$	Error log $\gamma_{Fe}^{Fe\text{-}Pt}$
		1400 °C, 1 atm		
6	0.1930	0.0173	−2.319	0.040
8	0.4320	0.0017	−1.170	0.002
11	0.0043	0.0008	−3.331	0.083
12	0.6405	0.0039	−0.509	0.003
13	0.5502	0.0045	−0.715	0.004
15	0.5477	0.0028	−0.713	0.002
16	0.2676	0.0067	−1.894	0.011
17	0.5636	0.0148	−0.687	0.012
20a	0.0044	0.0006	−3.345	0.061
20b	0.0044	0.0001	−3.345	0.011
21a	0.0506	0.0114	−3.051	0.010
21b	0.0422	0.0061	−2.972	0.064
23a	0.2293	0.0031	−2.203	0.006
23b	0.2308	0.0029	−2.206	0.006
vol. 1	0.3233	0.0042	−1.609	0.006
vol. 2	0.2332	0.0024	−2.084	0.005
vol. 3	0.4343	0.0030	−1.172	0.003
		1400 °C, 20 kbar		
P.C. 9	0.0122	0.0008	−3.839	0.030
P.C. 17a	0.3312	0.0046	−1.624	0.006
P.C. 17b	0.3195	0.0046	−1.608	0.007
		1300 °C, 1 atm		
18	0.2884	0.0198	−2.213	0.030
22a	0.0306	0.0126	−3.602	0.191
22b	0.0251	0.0031	−3.516	0.055
24a	0.2309	0.0018	−2.437	0.004
24b	0.2350	0.0011	−2.444	0.004
		1300 °C, 20 kbar		
P.C. 7	0.0237	0.0011	−4.193	0.021
P.C. 10	0.0274	0.0015	−4.256	0.025
P.C. 14a	0.4045	0.0090	−1.589	0.010
P.C. 14b	0.3791	0.0085	−1.561	0.010

Note: sd = 1 sd of the analytical data, error log $\gamma_{Fe}^{Fe\text{-}Pt}$ = uncertainty based on the analytical error and the error in Equation 1; a = pure Pt wire, b = presaturated Fe-Pt alloy.

The activity of Fe in the Fe-Pt alloy was calculated using the method of Darken and Gurry (1945) (Eq. 1), relative to a standard state of pure γ-Fe in equilibrium with wüstite. The calibration of Darken and Gurry (1945) compares very well with the calibration of O'Neill (1988), at the temperature of interest and 1 atm. The error in the activity coefficient, on the basis of normal propagation of the error in the activity of Fe in the iron oxides (from Darken and Gurry, 1945), and the error in the mole fraction of Fe in the Fe-Pt alloy (1 sd) are also shown in Table 3. The results are shown in Figure 3, a plot of log $\gamma_{Fe}^{Fe\text{-}Pt}$ vs. the mole fraction of Fe in the alloy.

The results of the 20-kbar experiments are also given in Table 3 and shown in Figure 3. The experiments conducted at f_{O_2} controlled by the WM buffer assembly show very little effect of pressure on the activity coefficient. In contrast, the experiments performed at MH f_{O_2} conditions show a significant pressure effect on the activity coefficient.

Four experiments (vol. 1, vol. 2, vol. 3, and vol. 4a,b) were performed at 1400 °C and 1 atm over a range of f_{O_2} and unit-cell parameters of the alloys determined by X-ray diffraction. The data are plotted in Figure 4. The data for the pure end-members shown in Figure 4 were taken from Robie et al. (1978). The measured volumes of the Fe-Pt

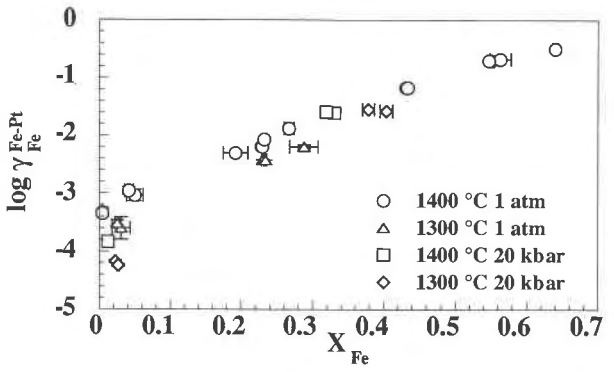

Fig. 3. Activity coefficient of Fe in Fe-Pt alloys vs. mole fraction of Fe at 1300 and 1400 °C and at 1 atm and 20 kbar. The horizontal error brackets represent ±1 sd of the analytical data, and the vertical error brackets represent combined error on the measured activity coefficients.

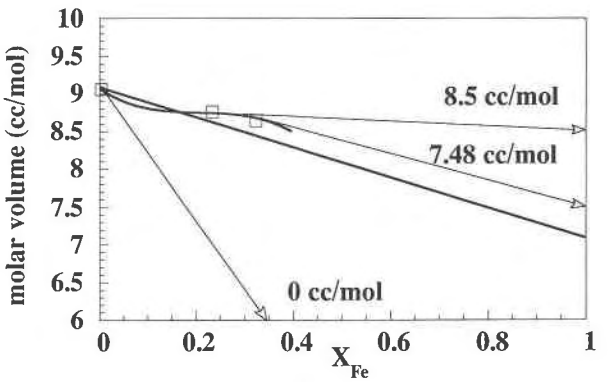

Fig. 4. Molar volume of Fe-Pt alloy at 25 °C and 1 atm vs. mole fraction of Fe. The boxes are measurements taken at 1 atm; the error bars are smaller than the symbols. The light lines with arrows show three different values for partial molar volume of Fe in the Fe-Pt alloys. See text for discussion.

alloys equilibrated in air are slightly less (9.06 ± 0.05 cc/mol) than is obtained from linear extrapolation between the pure end-members (9.08 cc/mol); however, within the error of the measurements, nonlinearity cannot be demonstrated. At intermediate f_{O_2} the measured volumes show a positive deviation from ideality. These measurements are consistent with the results of the 20-kbar experiments, both at 1300 and 1400 °C. Under very oxidized conditions (low X_{Fe}), the activity coefficient of Fe in the alloy decreases with increasing pressure. From the relationship

$$\frac{\partial \log \gamma_{Fe}}{\partial P} = \frac{V_{Fe} - v_{Fe}}{2.303\ RT} \tag{3}$$

where V_{Fe} and v_{Fe} are the partial molar volume of Fe in the alloy and the molar volume of the pure Fe end-member, respectively, the partial molar volume of Fe can be calculated. In order to explain the difference between the values of the activity coefficient at 1 atm and at 20 kbar, the partial molar volume of Fe in the alloy (at low X_{Fe}) must be about zero. The measured volume at low Fe contents of the alloy suggests that the volume-composition relationships do show a negative deviation from ideality. This is illustrated on Figure 4, the lowest arrow showing the partial molar volume of Fe in the alloy at very oxidized conditions. At intermediate f_{O_2}, the measured volumes show positive deviations from ideality, and between X_{Fe} of about 0.1 and 0.35, the partial molar volume of Fe in the Fe-Pt alloy remains constant at about 8.5 cc/mol. Measurement of the activity coefficient at WM shows a very small pressure effect, suggesting that the partial molar volume of Fe in the alloy is about 7.48 cc/mol. This is further illustrated on Figure 4, where the upper two lines show the partial molar volume of Fe at high values of X_{Fe}. At higher Fe content, it is likely that the volume-composition relationships become ideal.

The 1-atm data were fitted to the Redlich-Kister (R-K) solution model (Redlich and Kister, 1948):

$$Q = X_1(1 - X_1)[B + C(2X_1 - 1) + D(2X_1 - 1)^2 + \ldots] = \Delta G^E/2.303\ RT \tag{4}$$

where ΔG^E is the excess free energy, R is the universal gas constant, T is temperature in kelvin, X_1 is the mole fraction of Fe in the Fe-Pt alloy, and B, C, D, . . . are the R-K constants.

The R-K constants may be obtained from the expression

$$\log \gamma_1/\gamma_2 = dQ/dX = B(1 - 2X_1) + C[6X_1(1 - X_1) - 1] + D(1 - 2X_1)[1 - 8X_1(1 - X_1)] \tag{5}$$

since

$$Q = X_1 \log \gamma_1 + (1 - X_1)\log \gamma_2. \tag{6}$$

Given the composition dependence of $\log(\gamma_{Fe}/\gamma_{Pt})$, the values of the R-K constants can be derived for the Fe-Pt system at any given T and P. The activity coefficient of Pt was calculated from the experimentally derived values of γ_{Fe} with a Gibbs-Duhem integration:

$$d \log \gamma_{Pt} = -\int_{\substack{\log \gamma_{Fe} \\ \text{at } X_{Pt}=1}}^{\substack{\text{at } X_{Pt}=X_{Pt} \\ \log \gamma_{Fe}}} \frac{X_{Fe}}{X_{Pt}}\, d \log \gamma_{Fe}. \tag{7}$$

The R-K constants were then derived graphically from the composition dependence of $\log(\gamma_{Fe}/\gamma_{Pt})$. The results may be tested by applying the following condition:

$$\int_0^1 \log(\gamma_{Fe}/\gamma_{Pt})\, dX_{Fe} = 0. \tag{8}$$

This requirement is adequately fulfilled using only the first two constants in the R-K equation, which are at 1400 °C: $B = -3.5788$, and $C = -0.1510$. At 1300 °C, $B = -4.2019$, and $C = -0.3234$.

The activity coefficients of Fe and Pt in Fe-Pt alloy equilibrated at 1 atm may now be calculated as follows:

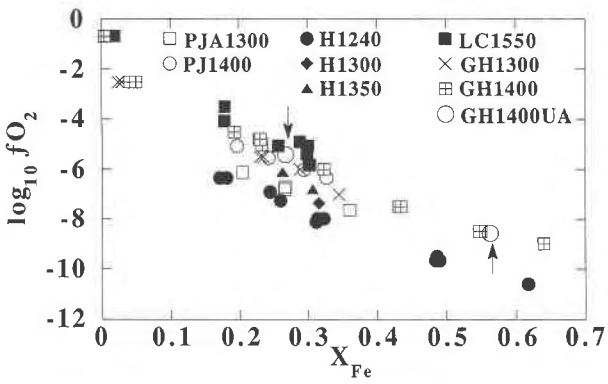

Fig. 5. Composition of Fe-Pt alloys for several experimental data sets. PJA is Petric et al. (1981), PJ is Petric and Jacob (1982), H is Heald (1967), LC is Larson and Chipman (1954), and GH is the present study. The arrows mark the two experiments done at the University of Arizona. The numbers in the legend refer to T in °C.

$$\log \gamma_{Fe} = Q + (1 - X)\frac{dQ}{dX}$$
$$= (1 - X_{Fe})^2[B + C(4X_{Fe} - 1)] \quad (9)$$

and

$$\log \gamma_{Pt} = Q - X\frac{dQ}{dX}$$
$$= X_{Fe}^2[B + C(4X_{Fe} - 3)]. \quad (10)$$

The error in the activity coefficient (γ) when calculated using Equations 9 and 10 is about ±6.5%, which is based on the error in the activity of Fe and the analytical error.

Discussion

Comparison with previous data

Figure 5 shows a comparison of our results with earlier data on a plot of the mole fraction of Fe in Pt vs. $\log_{10} f_{O_2}$. The two experiments performed at the University of Arizona were in perfect agreement with our study. In contrast, earlier data are more scattered. At 1300 °C, one data point from Heald (1967) coincides with the data of Petric et al. (1981), in which the samples contain less Fe in the alloy than we obtained. At low Fe content, the data of Petric and Jacob (1982) at 1400 °C fall very close to the data at 1300 °C in our study, but with increasing Fe content they approach our data at 1400 °C. The results of Larson and Chipman (1954) fall above all the other data sets and are very scattered. The differences among these studies can only be explained speculatively. With the assumption that in all of the earlier studies T and f_{O_2} were well controlled, it is likely that the difference lies within the analytical technique used. Analytical uncertainties were not reported in any of the previous studies, nor did any previous study use microbeam techniques for phase analysis. Also, none of the previous studies included reversal experiments, which allows for the possibility that equilibrium was not attained. In contrast, the present study is based on reversal experiments, microbeam analysis, and interlaboratory comparison.

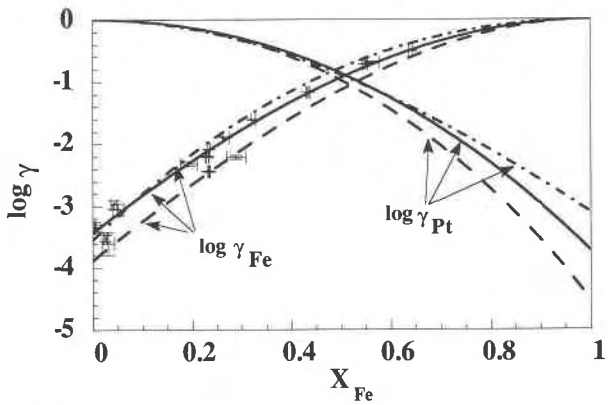

Fig. 6. Measured and calculated activity coefficients at 1300 and 1400 °C. The solid lines show the R-K model from this study at 1400 °C, the dashed lines represent the R-K model from this study at 1300 °C, and the dash-dotted lines show the R-K model of Heald (1967). The data shown are only from this study. The horizontal error brackets represent combined error in the measured activity coefficient.

Activity-composition relationship in the system Fe-Pt

Figure 6 illustrates the values of $\log_{10}\gamma_{Fe}$ in Fe-Pt alloy at 1300 and 1400 °C and 1 atm calculated using Equations 9 and 10 plotted against the mole fraction of Fe in the alloy. The data are well represented by the model for all compositions. Also shown in Figure 6 is the model of Heald (1967), which, as discussed above, is a polythermal fit to two data sets.

Calculations of f_{O_2} in high pressure experiments

As first noted by Bertka and Holloway (1988) and Gudmundsson et al. (1988), a sample in a high-pressure experiment consisting of olivine + orthopyroxene + Fe-Pt alloy reflects the value of f_{O_2} in the system. The f_{O_2} can be calculated by combining the IQF buffer reaction with the two silica buffer reactions as follows:

$$\underset{Fe}{2Fe} + \underset{melt}{SiO_2} + O_2 = \underset{olivine}{2FeSi_{0.5}O_2} \quad (11)$$

$$\underset{olivine}{2MgSi_{0.5}O_2} + \underset{melt}{SiO_2} = \underset{opx}{2MgSiO_3} \quad (12)$$

and

$$\underset{olivine}{2FeSi_{0.5}O_2} + \underset{melt}{SiO_2} = \underset{opx}{2FeSiO_3}. \quad (13)$$

The net reactions are

$$\underset{Fe}{2Fe} + \underset{opx}{2MgSiO_3} + O_2 = \underset{olivine}{2FeSi_{0.5}O_2} + \underset{olivine}{2MgSi_{0.5}O_2} \quad (14)$$

and

$$\underset{Fe}{2Fe} + \underset{opx}{2FeSiO_3} + O_2 = \underset{olivine}{4FeSi_{0.5}O_2}. \quad (15)$$

TABLE 4. Results of f_{O_2} test experiments

Expt.	$a^{opx}_{MgSiO_3}$	$a^{opx}_{FeSiO_3}$	$a^{olivine}_{MgSi_{0.5}O_2}$	$a^{olivine}_{FeSi_{0.5}O_2}$	a^{presat}_{Fe}	a^{pure}_{Fe}	log f_{O_2} (set)	log f_{O_2} (Eq. 16)	log f_{O_2} (Eq. 17)
I6	0.931	0.059	0.916	0.105	1.83×10^{-4}	2.56×10^{-4}	−4.50	−4.55 ± 0.1	−4.35 ± 0.1
I8	0.881	0.107	0.869	0.160	2.05×10^{-3}	2.45×10^{-3}	−6.00	−6.20 ± 0.1	−6.15 ± 0.1
I9	0.904	0.091	0.893	0.134	6.53×10^{-3}	5.58×10^{-3}	−7.50	−7.22 ± 0.1	−7.18 ± 0.1
B3	0.934	0.061	0.911	0.109	8.93×10^{-5}	7.06×10^{-5}	−3.70	−3.65 ± 0.1	−3.44 ± 0.1
B5	0.918	0.075	0.904	0.116	1.68×10^{-4}	1.08×10^{-4}	−4.06	−4.06 ± 0.2	−3.96 ± 0.2

The value of the f_{O_2} was calculated using the following calibrations, with the partial molar volume of Fe taken as 8.50 cc/mol:

$$\log_{10} f_{O_2} = 7.714 - \frac{29472}{T} + 0.054\frac{P-1}{T} + 2 \log a^{ol}_{MgSi_{0.5}O_2} - 2 \log a^{opx}_{MgSiO_3} + 2 \log a^{ol}_{FeSi_{0.5}O_2} - 2 \log a^{Fe\text{-}Pt}_{Fe} \quad (16)$$

and

$$\log_{10} f_{O_2} = 7.644 - \frac{29874}{T} + 0.051\frac{P-1}{T} + 4 \log a^{ol}_{FeSi_{0.5}O_2} - 2 \log a^{opx}_{FeSiO_3} - 2 \log a^{Fe\text{-}Pt}_{Fe} \quad (17)$$

where $a^{opx}_{MgSiO_3}$ and $a^{opx}_{FeSiO_3}$ are activities of enstatite and ferrosilite components in orthopyroxene, respectively, $a^{ol}_{MgSi_{0.5}O_2}$ and $a^{ol}_{FeSi_{0.5}O_2}$ are activities of forsterite and fayalite components in olivine, respectively, and $a^{Fe\text{-}Pt}_{Fe}$ is the activity of Fe in Fe-Pt alloy.

In order to test the applicability of our results, a series of experiments were performed at 1 atm and 1400 °C under controlled f_{O_2} ranging from $10^{-7.5}$ to $10^{-3.7}$. In these experiments, a 1921 Kilauea basalt was equilibrated with olivine, orthopyroxene, and Fe-Pt alloy. The activity of Fe in the alloy was calculated using Equation 9 to derive the activity coefficient, then the activity coefficient was multiplied by the mole fraction of Fe in the alloy, giving the activity of Fe in the alloy. The expression for the activity of $MgSi_{0.5}O_2$ and $FeSi_{0.5}O_2$ in olivine as a function of composition was taken from Wiser and Wood (1991), and the expression for the activity of $MgSiO_3$ and $FeSiO_3$ in orthopyroxene was taken from Ghiorso et al. (1983). The equilibrium constant for the IQF reaction (Eq. 11) was taken from O'Neill (1987b), and the equilibrium constant for Equations 12 and 13 was taken from Wood and Holloway (1984). The volume terms were taken from Robie et al. (1978).

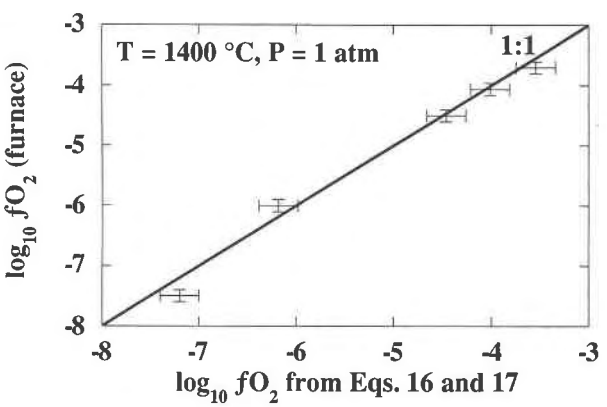

Fig. 7. Measured f_{O_2} determined from the olivine + orthopyroxene + Fe-Pt metal assemblage compared with the f_{O_2} fixed by CO/CO_2 gas mixtures at 1400 °C and 1 atm. The horizontal error brackets represent the combined error on the measured f_{O_2}, and the vertical error brackets show the total error on the set f_{O_2}.

The activities needed to calculate the value for f_{O_2} using Equations 16 and 17 are listed in Table 4. The value of $\log_{10} f_{O_2}$ was calculated with Equations 16 and 17. The results of the calculations are given in Table 4. The closeness of the fit of these two equations shows a very good internal consistency. Comparisons between the calculated and the set values are shown in Figure 7, where the average of the calculated values for f_{O_2}, shown in Table 4, vs. the experimental f_{O_2} are plotted. The error in the calculated f_{O_2} is about ± 0.2 $\log_{10}$ units, on the basis of the propagation of the error in the activity coefficient of Fe, the analytical error in the mole fraction of Fe in the Fe-Pt alloy, and the estimated error in the activities of forsterite and fayalite in olivine and enstatite and ferrosilite in orthopyroxene, with the error in f_{O_2} fixed by the CO/CO_2 gas mixture of about ± 0.10 $\log_{10}$ units. The calculated values of f_{O_2} are within the error of the experimental f_{O_2}, which means that, with this technique, the value for the f_{O_2} can be calculated to within ± 0.2 $\log_{10}$ units. This is a somewhat smaller average error than that found by Jamieson et al. (1992) using Heald's (1967) activity-composition relationship for Fe-Pt alloys.

CONCLUSIONS

The activity-composition relationships in the system Fe-Pt have been studied extensively at 1300 and 1400 °C and 1 atm and are shown in Figure 8. This figure clearly demonstrates the large negative deviation from ideality in the Fe-Pt system. Our results agree fairly well with previous studies, especially with Heald's (1967) work, but the new data clearly show a temperature dependence of the activity coefficient of Fe in the alloy. The pressure effect on the activity coefficient has also been investigated

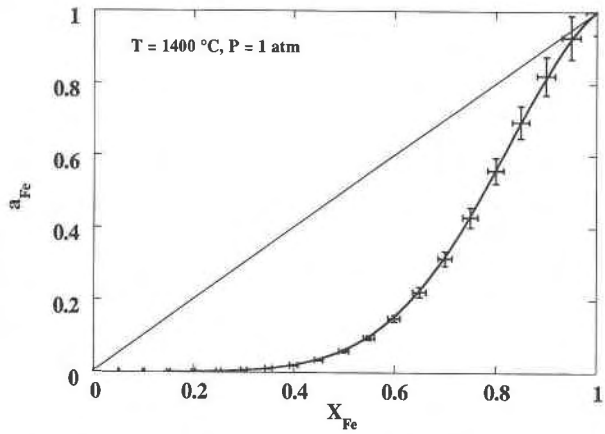

Fig. 8. The activity-composition relationship in the Fe-Pt system at 1400 °C and 1 atm. The vertical error brackets represent the total error on the calculated activity of Fe in the alloy, and the horizontal error brackets represent 1 sd of typical analyses of alloys by electron microprobe. The solid line shows the activity-composition relation for an ideal mixture.

at 20 kbar at 1300 and 1400 °C. At very low Fe contents, our results show that the volume of the alloy has a large negative deviation from ideality, but with increasing Fe content, the volume becomes ideal and, with further increase in the Fe content, the volume shows a positive deviation from ideality. With X_{Fe} ranging from 0.1 to about 0.35, the partial molar volume of Fe in the alloy remains essentially constant, at about 8.5 cc/mol. This range in X_{Fe} is a typical range in high-pressure experiments, and over this range in composition the f_{O_2} changes by almost 4 $\log_{10}$ units (Gudmundsson and Holloway, in preparation). At higher Fe contents, the volume-composition relationships become more ideal.

In high-pressure and high-temperature experiments it can be very difficult to control the f_{O_2}, the conventional way being to use solid buffers. An alternative approach is not to impose f_{O_2}, but to calculate its value at the end of the experiment from an appropriate coexisting phase assemblage. In this study, the IQF buffer reaction was used to calculate f_{O_2} at 1400 °C and 1 atm, with the activity of Fe being calculated using the model derived in this study. Gas-mixing experiments show that with this technique, the calculated f_{O_2} is accurate to within ± 0.2 $\log_{10}$ units.

One way to reduce Fe loss in high-pressure experiments is to presaturate the Pt container with Fe at 1 atm at an appropriate f_{O_2}. In order to achieve the best results, one must have a fairly good idea of what f_{O_2} conditions will prevail during the high-pressure experiment. The Pt container can then be presaturated at 1 atm using the same starting material at the same temperature and f_{O_2} as the high-pressure experiment. The duration of the presaturation should be about the same as the duration of the high-pressure experiment. Using this technique, the Fe loss in near liquidus or basaltic melt experiments is typically less than 5 wt% relative to the FeO (Gudmundsson, 1989).

Acknowledgments

Many thanks to Dave Joyce and Rick Hervig for helpful advice and discussions during the course of this study. This paper also benefited greatly from discussions with James A. Tyburczy and Simon M. Peacock. Reviews by two anonymous reviewers and Mark S. Ghiorso are gratefully acknowledged. Thanks are also due to Jim Clark, who provided assistance with the electron microprobe and to Ann Yates for her help with the XRD analysis. Mike Drake is thanked for the use of his laboratory at University of Arizona and Chris Capobianco is thanked for his assistance in performing these experiments. Finally, this work was greatly improved by discussions with Bernard J. Wood and by his revisions of the manuscript. The electron microprobe was purchased with the aid of NSF grant EAR-8408163. This study was supported by NSF grant EAR-8904261 to J.R.H. and NERC grant GR3/7142 to B.J. Wood.

References cited

Agee, C.B., and Walker, D. (1988) Static compression and olivine flotation in ultrabasic silicate liquid. Journal of Geophysical Research, 93, 3437–3449.

Berman, R.G. (1988) Internally-consistent thermodynamic data for minerals in the system Na_2O-K_2O-CaO-MgO-FeO-Fe_2O_3-Al_2O_3-SiO_2-TiO_2-H_2O-CO_2. Journal of Petrology, 29, 445–552.

Bertka, C.M., and Holloway, J.R. (1988) Martian mantle melts: An experimental study of iron-rich garnet lherzolite minimum melt composition. Proceedings of the 18th Lunar and Planetary Science Conference, p. 723–739. Cambridge University Press, Cambridge, U.K.

Biggar, G.M. (1970) Molybdenum as a container for melts containing iron-oxide. Bulletin of the American Ceramic Society, 49, 286–288.

Blumenthal, R.N., and Whitmore, D.H. (1961) Electrochemical measurements of elevated-temperature thermodynamic properties of certain iron and manganese oxide mixtures. Journal of the American Ceramic Society, 44, 508–512.

Darken, L.S., and Gurry, R.W. (1945) The system iron-oxygen. I. The wüstite field and related equilibria. Journal of the American Chemical Society, 67, 1398–1412.

——— (1946) The system iron-oxygen. II. Equilibrium and thermodynamics of liquid oxide and other phases. Journal of the American Chemical Society, 68, 798–816.

Esperanca, S., and Holloway, J.R. (1986) The origin of high-K latites from Camp Creek, Arizona: Constraints from experiments with variable f_{O_2} and aH_2O. Contributions to Mineralogy and Petrology, 93, 504–512.

Ford, C.E. (1978) Platinum-iron alloy sample containers for melting experiments on iron-bearing rocks, minerals and related systems. Mineralogical Magazine, 42, 271–275.

Ghiorso, M.S., Carmichael, I.S.E., Rivers, M.L., and Sack, R.O. (1983) The Gibbs free energy of mixing of natural silicate liquids; an expanded regular solution approximation for the calculation of magmatic intensive variables. Contributions to Mineralogy and Petrology, 84, 107–145.

Green, D.H., and Ringwood, A.E. (1967) The genesis of basaltic magmas. Contributions to Mineralogy and Petrology, 15, 103–190.

——— (1970) Mineralogy of peridotitic compositions under upper mantle conditions. Physics of the Earth and Planetary Interiors, 3, 359–371.

Grove, T.L. (1981) Use of FePt alloys to eliminate the iron loss problem in 1 atmosphere gas mixing experiments: Theoretical and practical considerations. Contributions to Mineralogy and Petrology, 78, 298–304.

Gudmundsson, G. (1989) Pressure effect on the ferric/ferrous ratio in basaltic liquids, 52 p. M.S. thesis. Arizona State University, Tempe, Arizona.

Gudmundsson, G., Holloway, J.R., and Carmichael, I.S.E. (1988) Pressure effect on the ferric/ferrous ratio in basaltic liquids. Eos, 69, 1511.

Heald, E.F. (1967) Thermodynamics of iron-platinum alloys. Transactions of the Metallurgical Society of AIME, 224, 1337–1340.

Holloway, J.R., Vivian, P., and Gudmundsson, G. (1992) Melting experiments in the presence of graphite: Oxygen fugacity, ferric/ferrous ratio and dissolved CO_2. European Journal of Mineralogy, 4, 105–114.

Hultgren, R., Desai, P.D., Hawkins, D.T., Gleider, M., and Kelly, K.K. (1973) Selected values of the thermodynamic properties of binary alloys. ASM International, Metals Park, Ohio.

Ito, K., and Kennedy, G.C. (1967) Melting and phase relations in a natural peridotite to 40 kilobars. American Journal of Science, 265, 519–538.

Jamieson, H.E., Roeder, P.L., and Grant, A.H. (1992) Olivine-pyroxene-PtFe alloy as an oxygen geobarometer. Journal of Geology, 100, 138–145.

Jeanloz, R., and Hazen, R.M. (1983) Compression, nonstoichiometry and bulk viscosity of wüstite. Nature, 304, 620–622.

Johannes, W., and Bode, B. (1978) Loss of iron to the Pt-container in melting experiments with basalts and a method to reduce it. Contributions to Mineralogy and Petrology, 67, 221–225.

Larson, H.R., and Chipman, J. (1954) Activity of iron in iron-platinum solid solutions. Acta Metallurgica, 2, 1–2.

Merrill, R.B., and Wyllie, P.J. (1973) Iron absorption by platinum capsules in high pressure rock melting experiments. American Mineralogist, 58, 16–20.

O'Neill, H.St.C. (1987a) Free energies of formation of NiO, CoO, Ni_2SiO_4, and Co_2SiO_4. American Mineralogist, 72, 280–291.

——— (1987b) Quartz-fayalite-iron and quartz-fayalite-magnetite equilibria in the free energy of formation of fayalite (Fe_2SiO_4) and magnetite (Fe_3O_4). American Mineralogist, 72, 67–75.

——— (1988) Systems Fe-O and Cu-O: Thermodynamic data for the equilibria Fe-"FeO," Fe-Fe_3O_4, "FeO"-Fe_3O_4, Fe_3O_4-Fe_2O_3, Cu-Cu_2O, and Cu_2O-CuO from emf measurements. American Mineralogist, 73, 470–486.

Patera, E.S., and Holloway, J.R. (1978) A non-endloaded piston cylinder design for use to forty kilobars. Eos, 59, 1217–1218.

Petric, A., and Jacob, K.T. (1982) Thermodynamic properties of Fe_3O_4-FeV_2O_4 and Fe_3O_4-$FeCr_3O_4$ spinel solid solutions. Journal of the American Ceramic Society, 65, 117–122.

Petric, A., Jacob, K.T., and Alcock, C.B. (1981) Thermodynamic properties of Fe_3O_4-$FeAl_2O_4$ spinel solid solutions. Journal of the American Ceramic Society, 64, 632–639.

Redlich, O., and Kister, A.T. (1948) Algebraic representation of thermodynamic properties and the classification of solutions. Industrial and Engineering Chemistry, 40, 345–348.

Reed, S.J.B. (1975) Electron microprobe analysis. Cambridge University Press, Cambridge, U.K.

Robie, R.A., Hemingway, B.S., and Fisher, J.R. (1978) Thermodynamic properties of minerals and related substances at 298.25 K and 1 bar (10^5 Pascal) pressure and at higher temperatures. U.S. Geological Survey Bulletin, 1452, 1–456.

Sato, M. (1970) An electrochemical method of oxygen fugacity control of furnace atmosphere for mineral synthesis. American Mineralogist, 55, 1424–1431.

Spencer, P.J., and Kubaschewski, O. (1978) A thermodynamic assessment of the iron-oxygen system. CALPHAD, 2, 147–167.

Stern, C.R., and Wyllie, P.J. (1975) Effect of iron absorption by noble-metal capsules on phase boundaries in rock-melting experiments at 30 kilobars. American Mineralogist, 60, 681–689.

Takahashi, E., and Kushiro, I. (1983) Melting of a dry peridotite at high pressure and basalt magma genesis. American Mineralogist, 68, 859–879.

Taylor, D. (1984) Thermal expansion data: I. Binary oxides with sodium chloride and wurtzite structures, MO. Journal of British Ceramic Transactions, 83, 5–9.

Taylor, R.W., and Muan, A. (1962) Activities of iron-platinum alloys at 1300 °C. Transactions of the Metallurgical Society of AIME, 224, 500–502.

Wiser, N.M., and Wood, B.J. (1991) Experimental determination of activities of Fe-Mg olivines at 1400 K. Contributions to Mineralogy and Petrology, 108, 146–163.

Wood, B.J., and Holloway, J.R. (1984) A thermodynamic model for subsolidus equilibria in the system CaO-MgO-Al_2O_3-SiO_2. Geochimica et Cosmochimica Acta, 48, 159–176.

Yoder, H.S., and Tilley, C.E. (1962) Origin of basalt magmas: Experimental study of natural and synthetic rock systems. Journal of Petrology, 3, 342–532.

Manuscript received March 7, 1991
Manuscript accepted July 9, 1992